Urban Climate 44 (2022) 101207

Contents lists available at ScienceDirect

Urban Climate

journal homepage: www.elsevier.com/locate/uclim

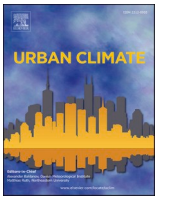

Characterization of the UHI in Zaragoza (Spain) using a quality-controlled hourly sensor-based urban climate network

Samuel Barrao [a,b,*], Roberto Serrano-Notivoli [c], José M. Cuadrat [a,b], Ernesto Tejedor [d], Miguel A. Saz Sánchez [a,b]

[a] Departamento de Geografía y Ordenación del Territorio, Universidad de Zaragoza, C. Pedro Cerbuna 12, 50009 Zaragoza, Spain
[b] Instituto Universitario de Investigación en Ciencias Ambientales de Aragón (IUCA), Universidad de Zaragoza, C. Pedro Cerbuna 12, 50009 Zaragoza, Spain
[c] Departamento de Geografía, Universidad Autónoma de Madrid, C. Francisco Tomás y Valiente 1, 28049 Madrid, Spain
[d] Department of Atmospheric and Environmental Sciences, University at Albany (SUNY), 1400 Washington Avenue, Albany, NY 12222, USA

ARTICLE INFO

Keywords:
Urban climate
Urban heat Island
Urban climate network
Quality control
Synoptic situations

ABSTRACT

The study of the urban heat island (UHI) is of great importance in the context of climate change, where increasingly frequent and intense extreme thermal events will generate lethal effects in cities. In this work, we characterize the UHI of the urban area of Zaragoza (Spain) using a thermohygrometric network of hourly observatories composed of 21 sensors, from March 2015 to February 2021. Due to the diversity of urban spaces and the high volume of information (≈ 995,000 observations), we performed an exhaustive quality control. Incorporating a synoptic analysis to better identify atmospheric situations not recorded by sensors. The results indicate that 1.6% of observations are removed, mainly due to outliers and hourly variability. We demonstrate that the UHI displays the classical center-periphery pattern with intensity values around 2 °C, but with variations due to the urban structure. We also observe seasonal UHI variations that intensify, especially in winter and autumn nights. Finally, this characterization confirms the differences in UHI intensity are due to their structural and climatic characteristics, which can ultimately guide the logical urban planning design of Zaragoza, and other Mediterranean-like cities with a similar urban environment.

1. Introduction

Urban areas occupy only about 1% of the world's land area (United Nations, 2019), and yet are home to around 55% of the world's population and are projected to increase substantially over the next ten years (Seto et al., 2010). This increase in urbanization and the concentration of population means that the inhabitants directly or indirectly modify their immediate environment, especially the climate (Bassett et al., 2016; Chen et al., 2020). Additionally, changes in land use have the potential to alter the surface energy balance and favor an increased difference between temperatures inside and outside the city (Oke, 1982).

Urban Heat Island (UHI) is a widely documented phenomenon (Arnfield, 2003; Masson et al., 2020; Oke, 1973, 1982; Stewart, 2011) that quantifies how urban areas are warmer than their rural surroundings. Previous studies addressed temperature differences of

* Corresponding author at: Departamento de Geografía y Ordenación del Territorio, Universidad de Zaragoza, C. Pedro Cerbuna 12, 50009 Zaragoza, Spain.
E-mail address: sbarrao@unizar.es (S. Barrao).

https://doi.org/10.1016/j.uclim.2022.101207
Received 1 December 2021; Received in revised form 22 March 2022; Accepted 28 May 2022
Available online 9 June 2022

up to 10 °C (Alcoforado et al., 2014; Warren et al., 2016) depending on the size of the city, urban morphology, land use, and specific weather conditions (Nastran et al., 2019; Peng et al., 2018; Yue et al., 2019). These differences occur mainly at night (Arnfield, 2003) when the energy absorbed by buildings and concrete surfaces during daytime is released to the atmosphere as heat. In addition, the structure and intensity of the UHI are defined by the city itself and often present spatial variations (Stewart and Oke, 2012).

The UHI phenomenon has potentially detrimental effects on the health of urban inhabitants. For instance, Heaviside et al. (2017) showed that health risks are higher in urban populations than in rural populations mainly during hot weather, an increasing risk that is aggravated during heatwave episodes (Royé et al., 2020). In other words, heat waves not only increase the temperature but also intensify the urban-rural temperature difference caused by UHI. The 2003 heat wave is estimated to have caused excess mortality in Europe of 70,000 people (Díaz Jiménez et al., 2006; García-Herrera et al., 2010; Garrabou et al., 2009), with the probability of death being higher in urban settings during this period (Heaviside et al., 2016; Laaidi et al., 2012). Given that these heat waves and tropical nights are expected to become increasingly frequent in the current climate change scenario (Cuadrat Prats et al., 2013; Olcina Cantos et al., 2019), it is important to highlight both the serious temperature-related health risks faced by urban populations in the 21st century, and to inform and improve adaptation and mitigation strategies to the negative effects of UHI. Thus, more detailed studies are needed to understand the heterogeneity of this phenomenon to reduce the impact and vulnerability of the urban population. However, such studies require rigorous information that covers the UHI from both a comprehensive temporal and spatial detailed perspective.

Traditionally, due to the scarce availability of sensors, urban studies were limited to comparing an urban sensor inside the city with an outdoor sensor in rural areas (Stewart, 2011). In many cases related to the metropolitan airport, a space that is not always representative of the rural environment. In others, urban transects are used with almost continuous temperature measurements over a specific period (Romero Rodríguez et al., 2020; Tsin et al., 2016). Different routes are made through the city to analyze the spatial configuration of the UHI. In the case of Zaragoza, the frequency and intensity of the phenomenon have been analyzed using this technique since 1990 (Cuadrat Prats et al., 1993, 2005, 2013, 2015; Saz Sánchez et al., 2003; Vicente Serrano et al., 2005). Although urban climate studies have improved significantly, the provision of atmospheric data from observation networks with high spatial

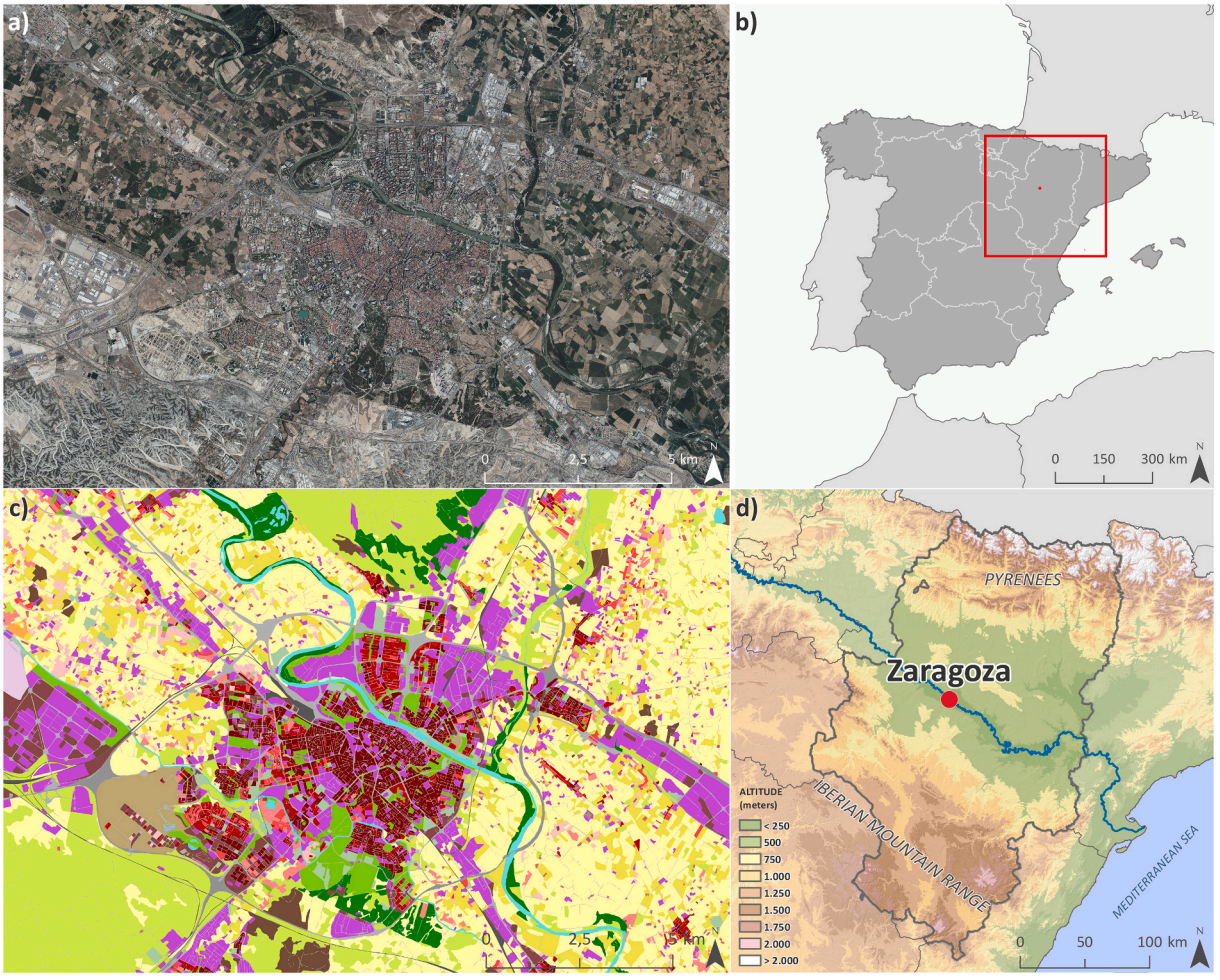

Fig. 1. Location of the city of Zaragoza. a) Aerial orthophoto, 2018 (Gobierno de España, 2018); b) Location within Spain (Instituto Geográfico Nacional, 2012); c) Urban land use map, 2018 (EEA, 2018); d) Location of Zaragoza and regional context.

resolution and over long periods of time remains a research challenge due to the difficulty in maintaining extensive networks over time, and the diversity of urban environments that condition the measurements. Some of the advances in this field have come from remote sensing and the possibility of studying surface temperature by using satellite or airborne thermal sensors (Voogt and Oke, 2003; Yue et al., 2019). However, such studies focus on the surface temperature of materials and not on the air temperature, being another area of investigation inside the UHI studies known as Surface Urban Heat Island (SUHI). Although they allow a detailed and continuous spatial resolution, this scale often does not fit in with the dimensions of medium or small cities, which fully depend on the number of pixels covering the urban area and therefore the heterogeneity of their different urban spaces is blurred. In addition, the lack of continuous information over time with very spaced return times and image availability, as well as the lack of data on the daily cycle, represents a real problem.

Traditional meteorological observation networks also have other drawbacks as they are designed for the detection of synoptic weather conditions, making them rarely suitable for urban or intra-urban specific analyses. Often, long and complete urban climate

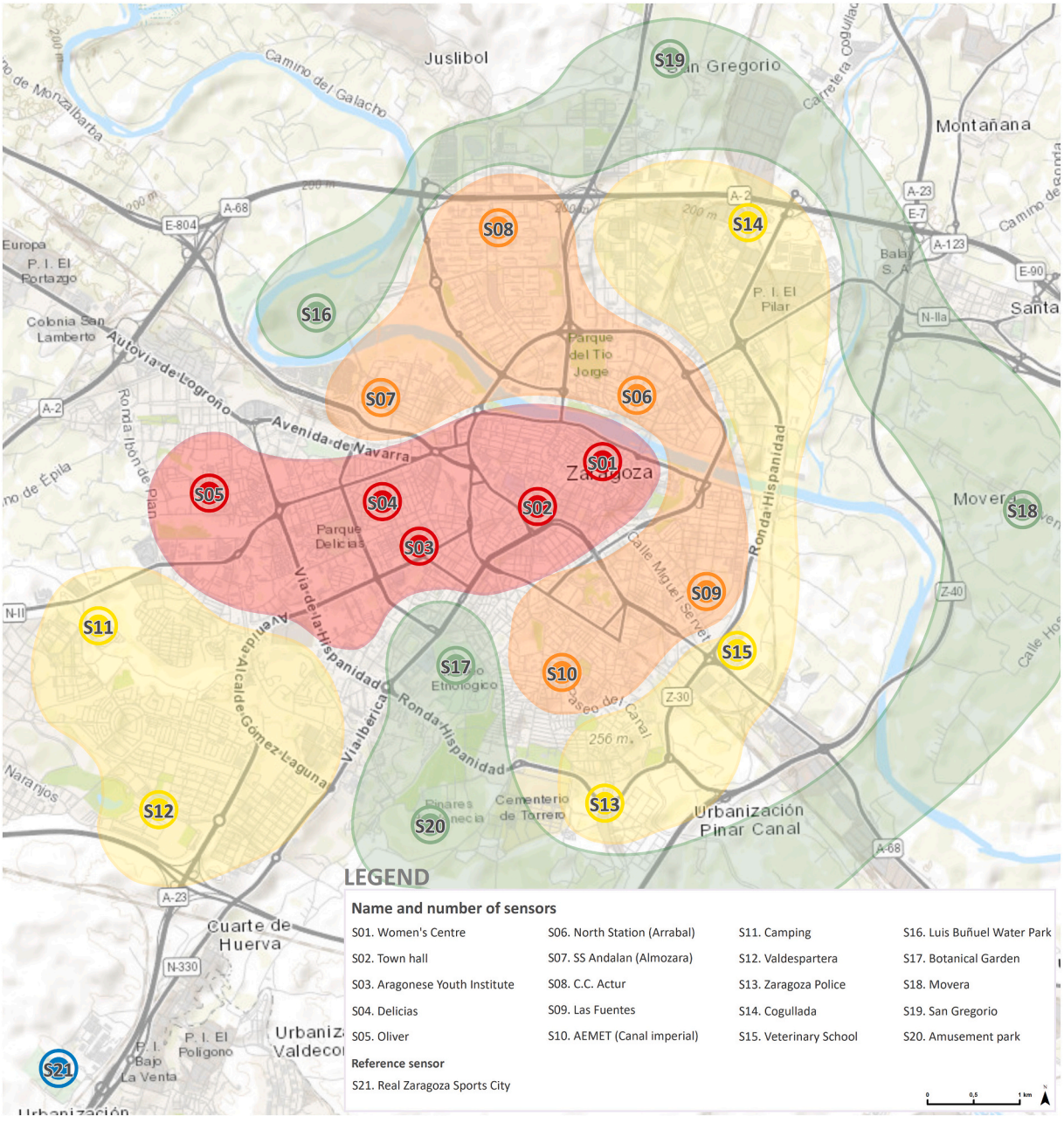

Fig. 2. Urban climate network in Zaragoza. Colors indicate the grouping based on their distance to the city center. S21 is used as non-urban reference.

data series source from outside the urban area (airports) and it is difficult to determine the true representativeness. Although many cities today have at least one station within their urban environment this is still deficient for a detailed analysis of the urban reality. Fortunately, a growing trend of urban meteorological network deployments is changing this situation (Bassett et al., 2016; Honjo et al., 2015; Smoliak et al., 2015; Vardoulakis et al., 2013; Warren et al., 2016). The development and progression of low-cost sensors and their proven quality offer new opportunities for urban networks (Meier et al., 2017), obtaining information at or below the hourly scale, which is key in urban climate studies.

Western Mediterranean areas, and especially the inland Iberian Peninsula (IP), exhibit a great climatic variability with very different regimes in relatively small areas with changes of frequency and magnitude in very short periods. It should be noted that the temperature monitoring network in Spain, under the responsibility of the State Meteorological Agency (AEMET), comprises more than 5000 stations over the last seven decades (Serrano-Notivoli et al., 2019), located mainly in natural areas (60.7%) and the rest (39.3%) in non-natural environments with a clear under-representation of the wide variety of urban areas, making it difficult to perform a comprehensive and representative analysis.

Here we present a new urban climate network in the city of Zaragoza (northeast Spain) based on 21 sensors monitoring temperature and humidity at high temporal resolution. Using hourly records from 2015 to 2020, we describe a thorough quality control process that allows us to identify: 1) measuring errors and 2) atmospheric situations such as advection fogs or convective storms. UHI patterns are described and analyzed in the context of urban morphology. Our study provides: 1) a new insight into the potential uses of high-resolution urban monitoring networks, using a case study of a medium-sized Mediterranean city; 2) a novel contribution in the measurement of UHI through an intra-urban scale climate analysis of different urban spaces; 3) a deep evaluation of the data quality and the possible sources of error, improving the usability of low-cost sensor networks in climate studies.

2. Study area

The city of Zaragoza is located in the northeast of the IP (Spain) (Fig. 1). It is the fifth-largest Spanish municipality with more than 714,000 inhabitants (2020) (Observatorio Municipal de Estadística, 2021), and the eighth largest urban area (Ministerio de Transporte, M. Y A.U, 2021). Within the European context, Zaragoza is a medium-sized regional metropolis, ranking among the top 100 cities in the European hierarchy (Rozenblat and Cicille, 2004). These types of medium and small cities are dominant in the European urban system, being of great importance in European spatial planning as they concentrate 22% of the total population of the continent, while large cities concentrate only 4% (Zdanowska et al., 2020).

Its location in the central area of the Ebro Depression at the confluence of the Ebro, Gállego, and Huerva rivers sets the physical and climatic features of the city. Its average altitude is 180 m a.s.l., and its topography does not present great contrasts. The climate of the area is Mediterranean with continental influence, with a predominance of anticyclonic situations during the summer and winter seasons (Cuadrat Prats et al., 1993, 2014, 2015). This continental character causes marked seasonal and daily temperature contrasts, reaching an average temperature oscillation of more than 10 °C in the summer months. The wind is another notable factor in the climate of Zaragoza. This frequent northwesterly wind reaches a high velocity due to the acceleration it undergoes as it is boxed into the Ebro Valley (Masson and Bougeault, 1996), and it is capable of reducing the urban heat island, even making it disappear at very high speeds (Lopes et al., 2013; Vicente Serrano et al., 2005).

3. Data

The urban climatic network consists of 21 sensors recording temperature and humidity which are distributed throughout the city and its closest suburban surroundings (Fig. 2). The maintenance of the sensors, data collection, and analysis are performed by the *Climate, Water, and Global Change* research group from the University of Zaragoza. The sensors are located in representative places of the most characteristic urban climatic environments, based on the Local Climate Zones (Stewart and Oke, 2012) to ensure that they are well represented. The 21 sensors cover a total of 11 different LCZs, with 7 built type classes and 4 land cover classes. The most represented typologies are urban categories ranging from compact to open with midrise to low-rise altitude as well as the large low-rise category. The sensors are HOBOpro v2 and HOBO MX2301 measuring devices recording temperature and humidity values on an hourly scale since March 2015 (Tejedor et al., 2016). Their operating range in temperature is from −40 °C to 70 °C and in humidity from 0 to 100%, with an accuracy of 0.21 °C and 2.5%, respectively, and a resolution of 0.02 °C in the case of temperature. They have a data-logger for storing information and a shelter to protect them from the direct solar radiation and the effect of rain.

Sensors have been grouped into four concentric rings (Fig. 2) according to the distance to the city center and broadly similar compact urban morphologies: The sensors closest to the inner city (S01 to S05) are located in densely urbanized spaces with little vegetation. The second (S06 to S10) and third (S11 to S14) groups are open spaces, with wider streets and more vegetation. However, they also include diverse urban spaces such as an industrial estate. The last group (S15 to S20) is composed of sensors located far from the city center, with little urbanization or with scattered buildings and a high presence of vegetation. The outermost sensor (S21) is used as a reference for the calculation of the Urban Heat Island and its intensity, being the sensor furthest away from the city center and placed in an open and clear space.

4. Methodology

The use of a network with such a dense spatial and temporal resolution results in very large databases in which we can identify different problems, such as missing data, outliers, or repetitions. Therefore, we considered as necessary the creation of a detailed

quality control procedure to identify potential errors and debug the flagged values. Such a method resulted in a reliable climatic database for the characterization of the UHI in Zaragoza.

4.1. Quality control

This section describes the quality control (QC) procedures to identify erroneous data from the sensors of the urban network (Fig. 3). The QC has been designed based on the recommendations of the World Meteorological Organization (WMO, 2017, 2018). In addition, to ensure the quality and accuracy of the data, we have included more restrictive criteria based on recent literature (Durre et al., 2008; Menne et al., 2012; Tomas-Burguera et al., 2016), taking into account the particularities involved in hourly climate databases (Beck et al., 2018; Lott, 2004) and, specifically, urban temperature and humidity data with very specific spatial characteristics.

Our QC generally involves automated processes to manage large hourly data sets, although some aspects, such as accounting for some errors in the hourly variation, manual intervention allows us to distinguish some errors from valid extreme data. Otherwise, these errors could be included in the database. The quality of the recorded data itself is also analyzed and checked, and those data that do not exceed the established thresholds as outliers or repeated data are disregarded. Therefore, a multilevel control approach has been used, consisting of procedures developed in the R programming language complemented with manual controls. In the following sections, each of the control steps developed in the methodology will be described and explained. The methodology is also shown in the scheme of the Fig. 3. Finally we obtained a high-quality, accurate and error-free urban climate database.

4.1.1. Detection of generic outliers

After data collection and the creation of a single database with homogeneous coding, the QC starts with the detection of outliers. Those values exceeding the climatic absolute physical limits are first eliminated. In the case of Zaragoza, due to its climatic characteristics, these limits are −15 °C and 50 °C for temperature and in the case of humidity the regular observational range, from 0% to 100%. This step applies the first general QC, but it does not allow a deep analysis of the outliers as well as it obviates the check of the

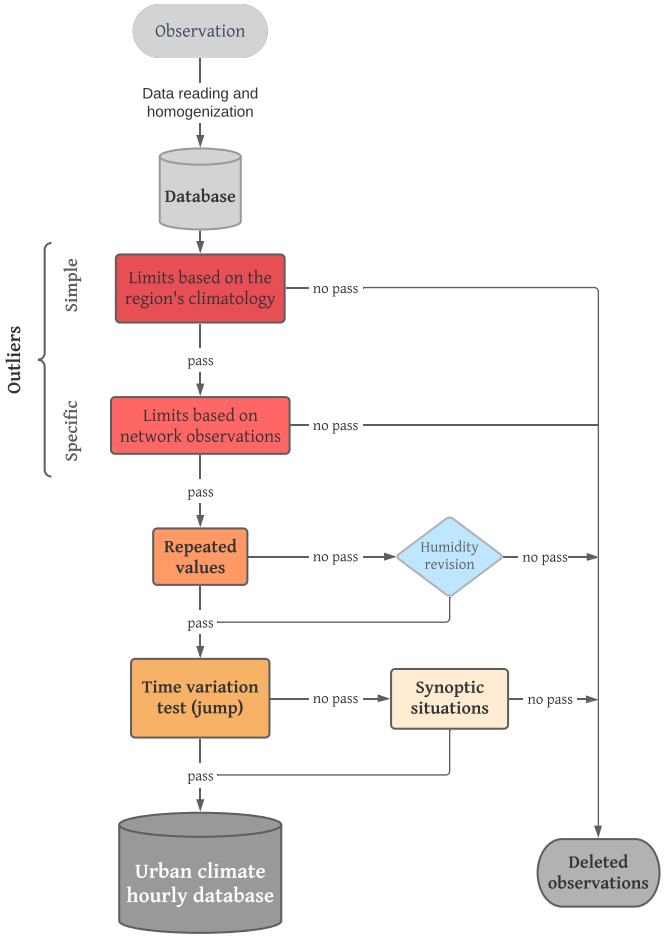

Fig. 3. Quality control flowchart describing all steps of the procedure.

inconsistencies that are hidden in the hourly, daily, and seasonal variation. For this reason, a tailored detection of outliers is needed.

4.1.2. Detection of specific outliers

The detection of outliers is a hard task with many uncertainties, especially when using automated procedures, and statistical analyses of data series provide useful resources to set thresholds with the aim of flag and remove unrealistic values. In this case, we used a $\pm$ 3 standard deviations to identify records not corresponding with the natural variability of the temperature or humidity series. The selection of this limit of 3 standard deviations is because it is a typical value as a multiplication factor for the detection of outliers (Beck et al., 2018; Velleman and Hoaglin, 1981). In addition, it is the tightest, since it was found that if lower values were used, numerous false positives were created by erroneously marking correct values as outliers. On the other hand, if the threshold was increased, it was so loose that registration errors went unnoticed and were included in the database.

4.1.3. Detection of abnormally repeated values

Repetition of a few consecutive values can be relatively common in automated sensors recording data in very short periods of time (e.g., hours). However, when these repetitions extend over long periods, they are often due to recording failures. Setting a number of repetitions as a threshold to identify erroneous data is challenging but, depending on the climatic characteristics and knowing the usual temperature and humidity cycles, an approximate number can be found (Serrano-Notivoli et al., 2017, 2019). We set 12 repetitions (same value in 12 consecutive hours) as a threshold because it is a period in which temperature and humidity should change even in extremely stable conditions (e.g., persistent fog, thermal inversions, etc.). However, due to persistent fog phenomena the humidity data detects more repetitions which requires a specific revision in order not to eliminate correct values.

4.1.4. Analysis of hourly variation or jump

To identify non-natural variations of temperature and humidity, the hourly variability of all measurements has been analyzed through the calculation of the difference between two consecutive values (*jumps*). The *jumps* are variable throughout the year, so we set $\pm$3 standard deviations as the threshold to flag suspicious values. Data exceeding this threshold were checked manually because not all suspicious data are due to non-natural errors, but may be due to specific meteorological situations causing abrupt hourly variations in the records. Thus, the daily synoptic situations were subsequently analyzed for all suspicious data to check whether they corresponded to atmospheric dynamics promoting rapid changes in the values or not.

4.1.5. Synoptic situations

Synoptic situations were estimated to help identify truly erroneous values, which required a synoptic classification to obtain the main atmospheric patterns. The R package "synoptReg" (Lemus-Canovas et al., 2019) was used, as it allows to obtain a synoptic climate classification of a given region. This analysis is based on atmospheric circulation types and NOAA NCEP/NCAR data reanalysis applying a PCA-based approach.

The synoptic situations were calculated for each day, and flagged as suspicious in the database based on jumps thresholds. Then, once the suspicious days were identified, a series of variables are downloaded for each of them and incorporated into the model for calculating synoptic situations. These variables are the mean sea level pressure, the geopotential height at 500 hPa, and the near-surface temperature since they together provide the most information without adding too much error to the model. The number of components that are incorporated into the PCA are four, representing approximately 80% of the explained variance. Providing a classification of 7 specific synoptic situations for these periods with suspicious data. A greater number of PCAs were not incorporated even though the variance explained increased and the number of synoptic situations was greater, since the situations obtained were slight variations that did not provide useful information in this type of study.

4.2. UHI characterization

The benefit of such a large number of stations is the possibility of detailing the climatic behavior in different areas of the city that would otherwise be difficult to represent. To characterize the effect of the UHI, the methodology is based on the comparison of data series recorded within the urban area with nearby rural series (Masson et al., 2020; Stewart, 2011), but it is necessary that the chosen stations have the appropriate characteristics for this type of study (Stewart and Oke, 2012), such as our extensive sensor-based network. Therefore, the urban stations are located in representative areas of the different urban spaces that make up the city and the rural station is outside the area of urban influence (Fig. 2). The latter sensor is located south of Zaragoza in a neighboring municipality and about 10 km of the urban center of the area study. In an open and controlled space where the urban effect and the UHI are not appreciable.

The objective of calculating the temperature difference as a characterization of the UHI in such a dense network of sensors is to be able to carry out an analysis in 2 dimensions: 1) Spatial, allowing a detailed analysis of the effect of urban morphology and the different spaces of the city (Huang and Wang, 2019; Salvati et al., 2019), not only from a theoretical point of view but also empirically with detailed data. This is achieved following the classical UHI studies, recently enhanced with the inclusion of satellite information. In this case, it is actually UHI and not SUHI as in remote sensing studies (Deilami et al., 2018); 2) Temporal: the time differentiation of UHI helps to understand its remarkable diurnal variability with different behavior during the day and night, leading to very different effects, including those affecting human health (Iñiguez et al., 2021; Royé et al., 2021).

To complement this analysis, the average daily and nocturnal UHI intensity for each sensor has been calculated for each season of the year to better evaluate the intensity of the urban effect at different times of the year. Regarding the delimitation of the daytime and

Table 1
Summary table with counts of original values of temperature and humidity, missing data, and data removed by QC, in absolute values and percentages for each sensor in the network.

	Sensors		Original database		Number of observations eliminated in the QC					Percentage of observations eliminated in QC				
Groups	Number	Name	Number of observations	Missing data	Simple outliers	Specific outliers	Repeated	Jumps	Total observations eliminated	Simple outliers	Specific outliers	Repeated	Jumps	Total observations eliminated
	S01	Women's Centre	52,080	778	2	54	0	0	56	0.004	0.1	0	0	0.1
	S02	Town hall	52,080	7830	0	37	0	198	235	0	0.08	0	0.4	0.5
1	S03	Aragonese Youth Institute	43,074	2	0	0	0	0	0	0	0	0	0	0
	S04	Delicias	52,080	7049	0	1	0	0	1	0	0.002	0	0	0.002
	S05	Oliver	43,074	2313	0	9	0	0	9	0	0.02	0	0	0.02
	S06	North Station	52,080	6079	258	855	0	0	1113	0.6	1.9	0	0	2.4
	S07	SS Andalan	43,074	4	0	2	0	0	2	0	0.005	0	0	0.005
2	S08	Actur	52,080	3124	0	10	0	0	10	0	0.02	0	0	0.02
	S09	Las Fuentes	52,080	9	0	22	0	0	22	0	0.04	0	0	0.04
	S10	AEMET	52,080	5	2196	605	0	0	2801	4.2	1.2	0	0	5.4
	S11	Camping	52,080	7	0	7	0	0	7	0	0.01	0	0	0.01
	S12	Valdespartera	52,080	6	0	2	0	0	2	0	0.004	0	0	0.004
	S13	Zaragoza Police	52,080	11	0	18	0	2048	2066	0	0.03	0	3.9	3.97
3	S14	Cogullada	43,074	7	0	6	0	0	6	0	0.01	0	0	0.01
	S15	Veterinary School	16,091	0	0	268	0	0	268	0	1.7	0	0	1.7
	S16	Luis Buñuel Park	52,080	7	0	63	0	0	63	0	0.1	0	0	0.1
	S17	Botanical Garden	52,080	5933	390	4169	0	34	4593	0.8	9.03	0	0.07	9.95
4	S18	Movera	52,080	5065	326	69	0	37	432	0.7	0.1	0	0.08	0.9
	S19	San Gregorio	52,080	7	0	226	0	0	226	0	0.4	0	0	0.4
	S20	Amusement park	24,806	4773	0	257	0	0	257	0	1.3	0	0	1.3
Reference sensor	S21	Real Zaragoza Sports City	52,080	4	738	1072	0	2048	3858	1.4	2.06	0	3.9	7.4
Total	**Total sensor network**		**994,393**	**43,013**	**3910**	**7752**	**0**	**4365**	**16,027**	**0.39**	**0.8**	**0**	**0.44**	**1.6**

nighttime period, it has been divided into nighttime (20:00-6:00) and daytime (10:00-18:00) (Alcoforado et al., 2014; Lopes et al., 2013). Wide margins allow both periods of the day to be clearly identified for all seasons, taking into account that during the most opposite seasons the time limits of sunrise and sunset vary. And the effects on temperature caused by shadows from buildings close to the sensors during the hours around sunset and sunrise are partially avoided (Alcoforado et al., 2014).

5. Results

5.1. Statistical quality control

Considering the full period of study, from March 2015 to February 2021, a total of almost one million hourly observations were recorded (994,393 observations). We found 4.3% of missing data, which can be explained due to sensor failures or sensor replacement and calibration periods (Table 1). After the application of the QC, the data flagged as suspicious and subsequently removed were 1.6% of the total number of observations.

The results after applying the QC procedures are as follows: i) the first QC step where basic thresholds were set for outlier detection removed 3910 hourly observations, representing 24% of the removed observations and 0.39% of the total network. Ii) The QC step related to the detection of specific outliers by thresholds, removed the largest number of observations, 7752, which represents 49% of the observations eliminated by QC and 0.8% of the raw observations. iii) The step related to jumps shows similar values with a detection of 4365 observations, 27% of the total number of eliminated values and 0.44% of the total network data. However, in this case, the particularity is that the error is concentrated in a smaller number of stations (Fig. 4). On the other hand, there were not repeated values recorded in the case of temperature. In the case of humidity, some suspicious repeated values were detected but dismissed as errors due to fog phenomena.

The temporal distribution of detected suspicious data (Fig. 5) shows that most of them were deleted at the beginning of the recording period (33.73% in the first year). There are as well erroneous data eliminated in the year 2018, that reach an average of 492 deleted observations per month in 2018, while the average for the whole series is 222 observations. On a monthly basis there is no specific period in the time series in which the number of deleted observations is concentrated, although there was a slight clustering in autumn and summer months. If we compare these deleted data with the total number of data available for that month, we observe that at the beginning of the implementation of the sensor network was when more deletions occurred. However, as the records progressed

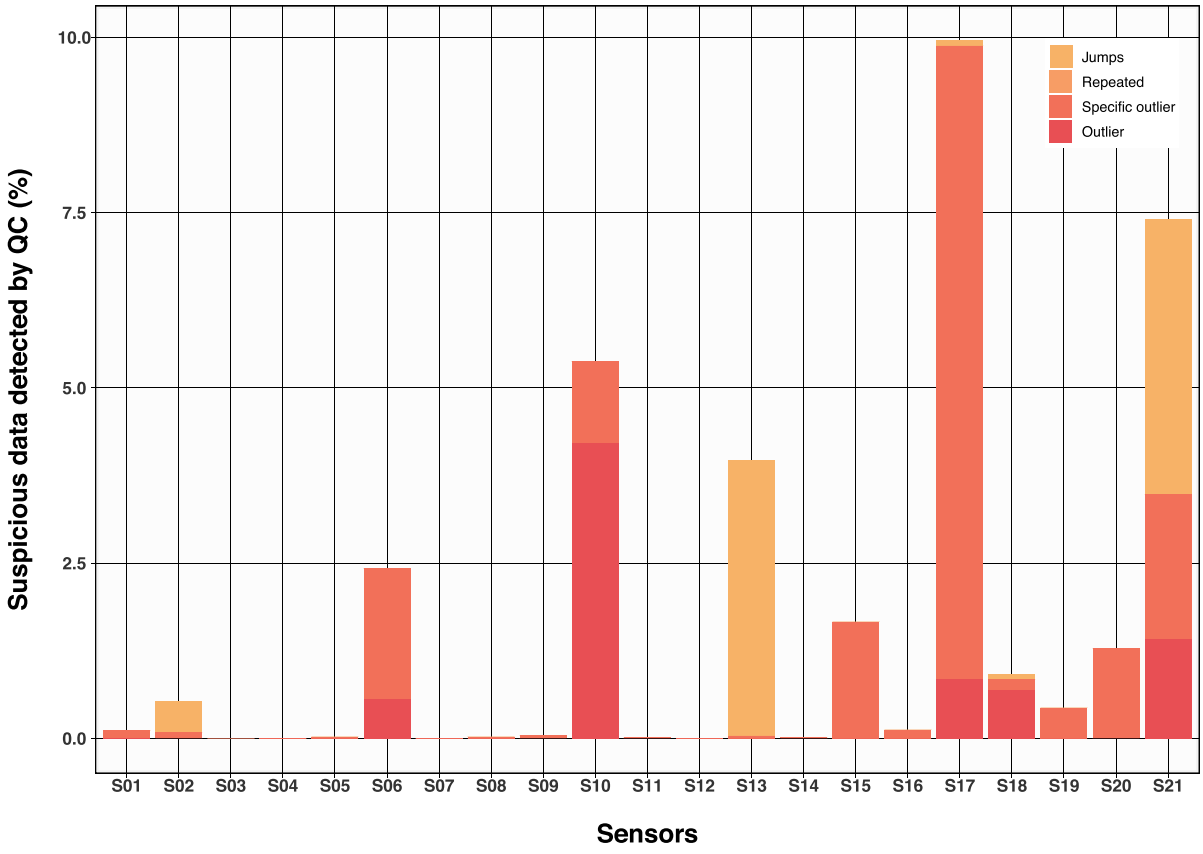

Fig. 4. Percentage of observations identified and eliminated from the original records for each sensor in the network.

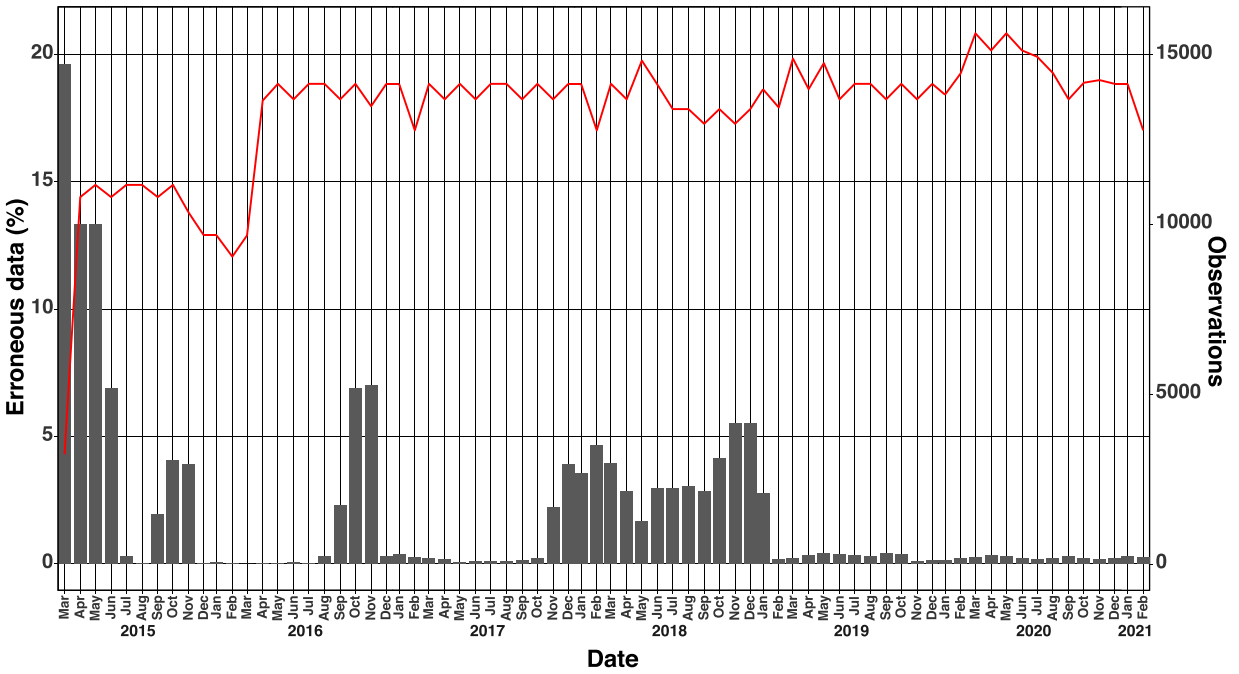

Fig. 5. Monthly evolution of the percentage of total observations eliminated and number of total data available for each month of the year.

and the network was supplemented with more sensors, these errors decreased. The average from 2016 onwards was less than 2.5% of deleted data for every 1400 observations, about 35 observations per month.

5.2. Synoptic attributions as a mean of QC

Seven synoptic situations were identified (Fig. 6) representing the most relevant circulation patterns in the IP in the period encompassing the dates catalogued as suspicious due to their excessive hourly variation (see Section 4.1.4.).

First, the typology ST1 (situation) is associated with a cyclonic situation with advection from the northwest. This type of situation, except for the summer months (JJA), can occur throughout the year, although in the results obtained it is concentrated in spring and winter. The Atlantic anticyclone is located over the Azores, which produces an upward displacement northwards. This causes mid-latitude depressions to skirt the anticyclone and become centered over the British Isles and northern Europe, introducing north-westerly air into the IP that leads to cold front sweeps across Spain with a generalized situation of showers over most of the territory, including Zaragoza.

The second typology ST2 is one of the most characteristic situations of the IP occurring mainly in winter, when a tropical air ridge settles over the IP, causing mild temperatures during the day, but cold nights due to the loss of daytime heat by irradiation. This thermal anticyclone situation causes low surface temperatures favoring stability and increased surface pressure. The resulting atmospheric situation promotes low temperatures, possible frost in the interior and morning fogs that extend in valley areas such as the Ebro valley where Zaragoza is located.

The third situation, ST3, shows some of the characteristics of situations of advection from east. High pressures over the European continent and Great Britain that in this case are somewhat more displaced towards the interior of the continent, favoring instability over the IP, even in favorable conditions at altitude, low pressure cells or cut-off low can be formed. In addition, it is a typology that is mainly concentrated in the spring and winter months.

ST4 corresponds to synoptic situations of advection from the west and has been registered mainly in the winter months. The weather associated with this situation is unstable in a large part of the peninsula due to the constant succession of fronts that cross the entire territory in a westerly direction, crossing the Ebro valley. Temperatures rise and fall after the passage of the fronts. Likewise, sunny weather alternates with cloudy and rainy weather, causing abundant precipitation associated with the passage of fronts.

The fifth situation, ST5, is mainly concentrated in spring and its surface distribution reflects an anticyclonic situation. The Azores anticyclone extends towards Europe producing sunny and warm weather due to the arrival of tropical air from the African continent, over which there is a thermal low probably related to the high temperatures in North Africa.

In the case of the ST6, it is concentrated in the summer months and resembles a cyclonic situation with advection from the southwest. In this type of situation, the location of a depression or isolated cold squall generates fronts that cross the peninsula from the southwest causing significant rainfall that can spread throughout the territory, affecting Zaragoza.

The ST7 and last of the categorized situations is similar to the thermal low or heat wave conditions. From all the situations, this is

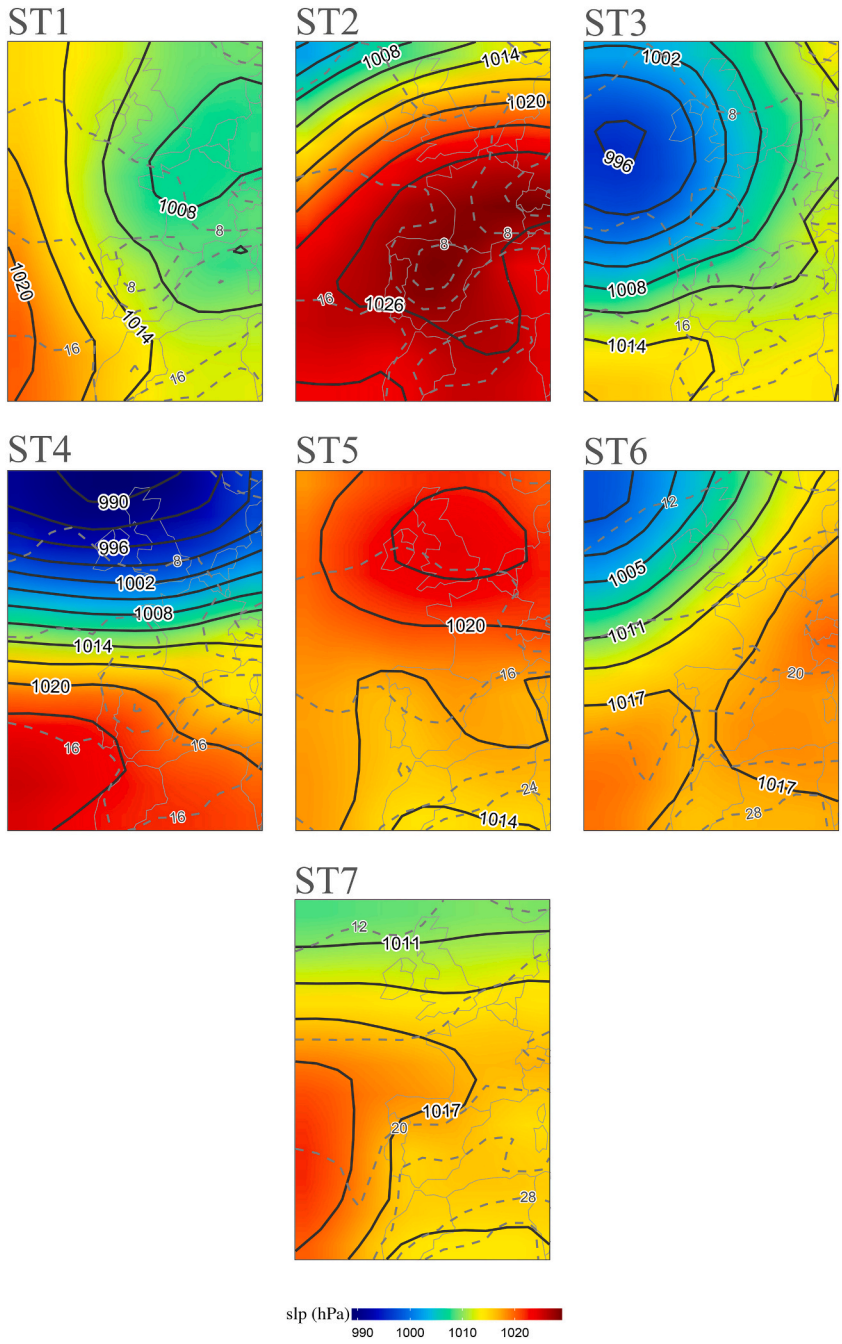

Fig. 6. Synoptic situations (1 to 7) categorized for those records marked as suspicious by the QC. Colors represent the sea level pressure (slp) in hPa, bold solid lines are isobars of the same variable, and surface temperature (°C) is represented by dashed lines.

the most frequent in summer months. It is characterized by a significant increase in temperatures caused by the entry of very warm air from North Africa. Despite the usual absence of precipitation, isolated but relatively common storms also occur.

Once all the typologies were calculated and identified, these synoptic situations were related to the observations catalogued as suspicious in the QC (Fig. 7). We obtained a series of patterns that allow us to differentiate whether these observations are due to specific situations or to measurement errors.

Thus, sharp positive changes in humidity are related to a decrease of temperature and, conversely, negative changes in humidity are associated with an increase in temperature. The greatest hourly temperature differences of the entire series were obtained in the months from June to August, sometimes exceeding decreases of −10 °C with humidity increases of more than 30%. The opposite occurred from December to February, with temperature increases of less than 10 °C associated with humidity decreases of −30%.

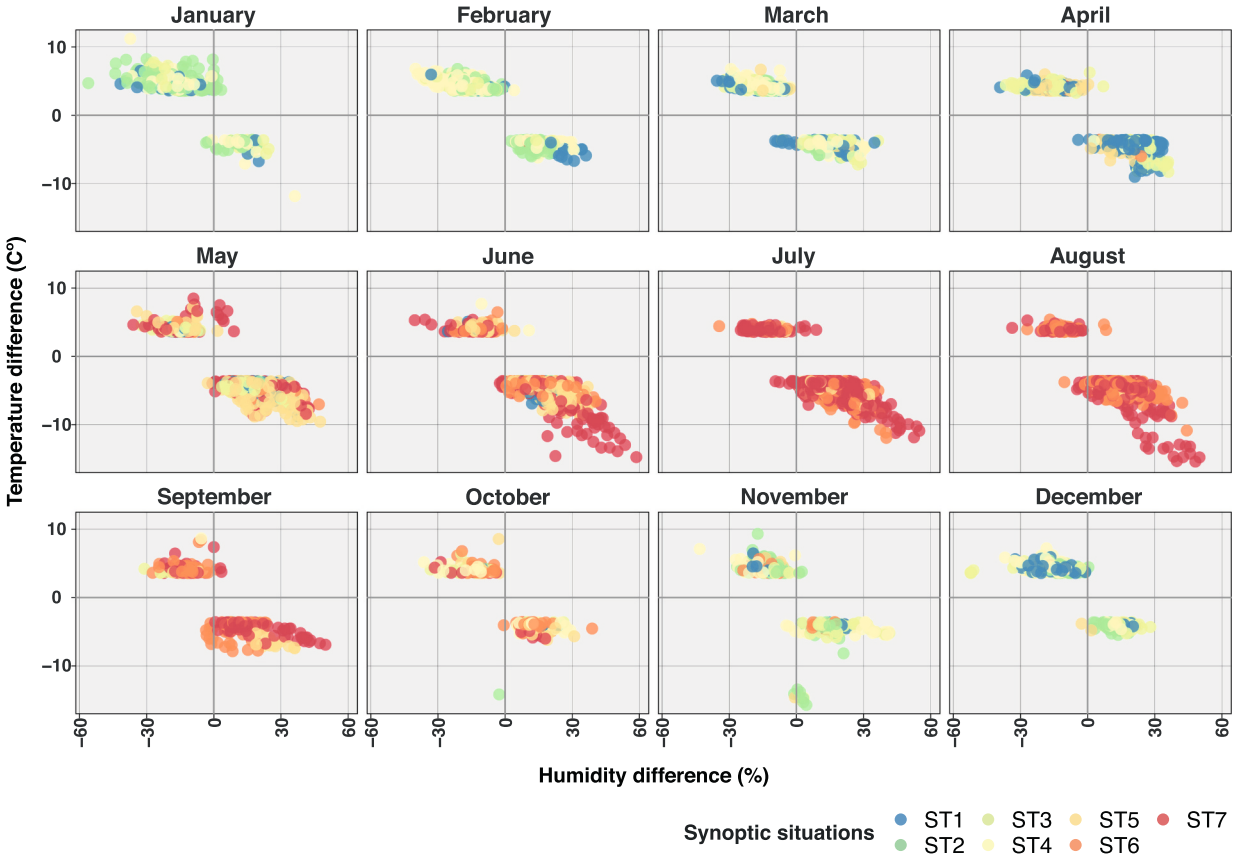

Fig. 7. Monthly distribution of suspicious observations detected QC and the associated synoptic situation typology by color. The x-axis represents the hourly variation in humidity and the y-axis represents the variation in temperature.

Certain atmospheric situations are related to specific errors and months. For instance, in warmer months, typologies 6 and 7 are the most frequent. This is due to summer thermal lows or heat waves (7) and to cyclonic situations with southwesterly advection (6). In both cases the occurrence of storms is relatively usual, but they are less common in type 7. These are events of great intensity in a short period of time, leading to temperature decreases of around 10 °C in one hour that are not due to a recording failure. It occurs during summer afternoons, after a steady rise in temperature throughout the day, a storm occurs that causes a temperature contrast, cooling the city very quickly and abruptly. This is reflected in the increase in humidity linked to this drop.

In winter, anomalies of temperature between hours can reach 5 °C to 10 °C. In this case, the predominant types of situations are not as specific as in the summer case, but types 2, 3 and 4 (winter thermal anticyclone, advection from the east, and advection from the west, respectively) are the most frequent. The highest anomalies reached in this period are concentrated in January under the situation of the thermal anticyclone. As explained above, this type of weather is characterized by mild daytime temperatures regarding the season, and cold nights. In the city of Zaragoza, this usually leads to early-morning frosts and thick and persistent fog banks that, when dissipated at midday, rapidly drop humidity and rise temperature. The succession of fronts interspersed with cloudy and clear skies, produces the same effect, as the insolation causes the warming of the city and the increase in the recorded temperature.

However, some of the detected anomalies in observations could not be explained neither by the atmospheric situation, nor by the time of the year, nor by the behavior of the humidity. Thus, they were identified as errors and eliminated from the database. These anomalies were observed mainly in the month of November, registering a notable decrease in temperature with minimal variation in humidity. Also, they correspond with situations 2, 4 and 5, that do not satisfactorily explain the reason of the decrease. The observations correspond to stations S17 and S18 in a period of the series in which both sensors had already had failures that had been eliminated in previous QC steps. Therefore, these erroneous observations correspond to observations that did not exceed the previous QC limits and that this new step of the more detailed control has allowed to identify.

Finally, after the manual control of the data, we also identified some *jump* errors that could not be explained by the atmospheric situations of sensors S13 and S21. These errors were occasional, but after the revision, a series of errors in the time evolution at the beginning of both series were noticed, so we eliminated the entire initial period.

Once this section was completed and these last identified errors were eliminated from the database thanks to the classification of synoptic situations, a filtered hourly database was obtained to proceed with the analysis and climatic characterization of the urban environment of the city of Zaragoza.

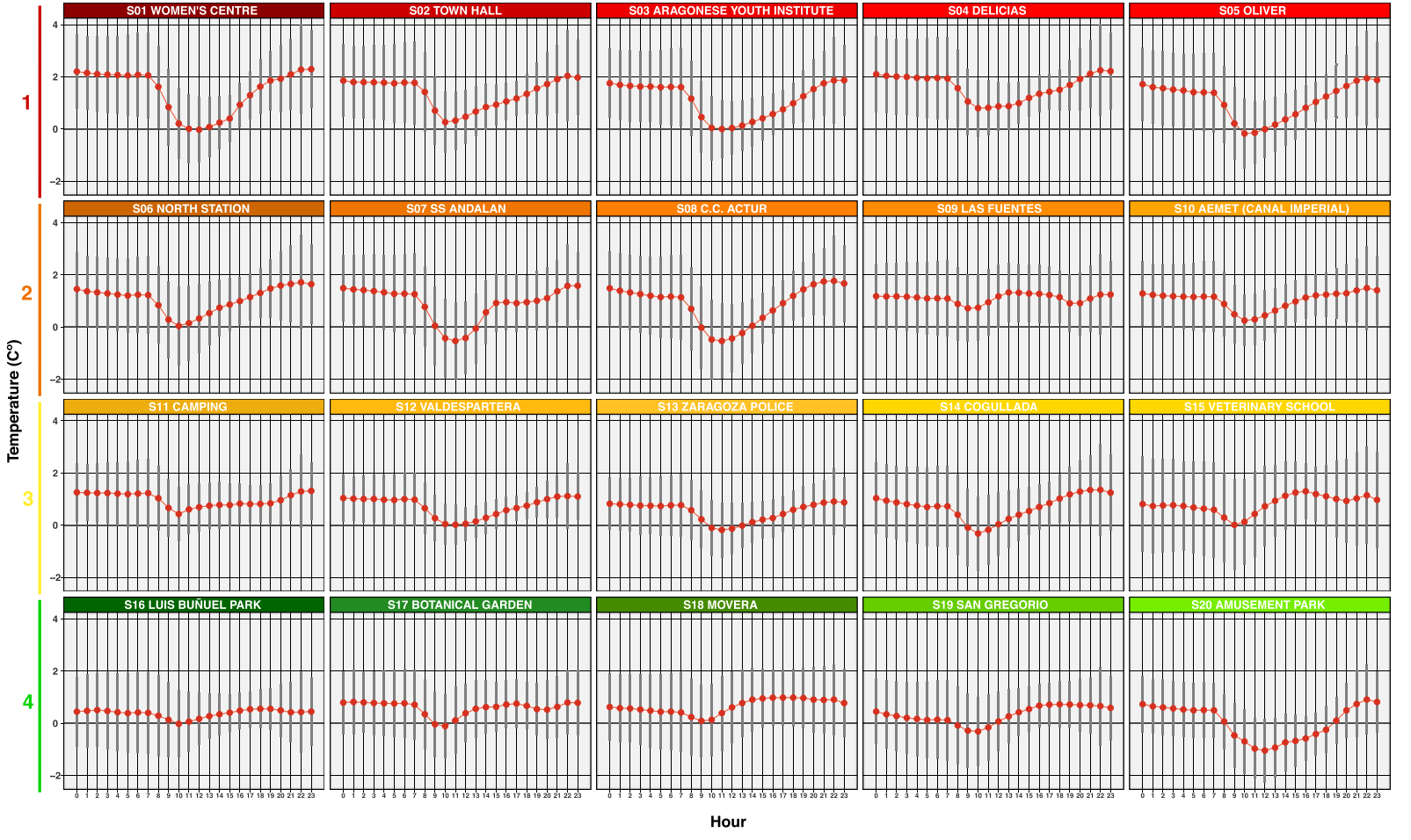

Fig. 8. Hourly UHI intensity per sensor. The hourly standard deviation is included to approximate the temperature variability. To the right and using the same color range the agraputions already marked in Fig. 2.

5.3. UHI characterization

The behavior of the temperature recorded in the different sensors shows diverse diurnal distributions of UHI (Fig. 8) but, in general terms, a number of common features can be observed. In all cases the UHI effect is visible by showing a positive intensity, being higher in specific moments of the day and locations in the city. It is during the night that the effect intensifies, while during the day the intensity decreases and the UHI even disappears when negative values are reached. This temporal distribution draws the U or V shape characteristic of this type of UHI graphs. The greater the urban effect, the sharper the differences and the more pronounced the U-shaped graph. Conversely, the effect is less pronounced when we are in the urban periphery or in large open green spaces of the city so that the shape of the graph becomes blurred and flattened. The UHI effect is most intense in stations near downtown, reaching about 2 °C on average and these shapes are generally U or V shaped (Fig. 8, rows 1 and 2). However, for sensors located in the periphery of the city and large metropolitan parks, the intensity rarely reaches 1 °C on average over the day, drawing a planar temporal distribution (Fig. 8, row 4).

The clearest example of the effect of UHI on city temperatures is the case of the sensor located downtown (S01), which is in a densely built-up area with medium-sized buildings and a very compact morphology of narrow, winding streets with little vegetation. This fits with the U-shaped distribution in the graph, with values around 0 °C in the central hours of the day and at night the intensity increases to over 2 °C until sunrise. Another similar case is the case of S04, one of the areas of the city with the highest urban density and population density, whose intensity is so high that it always registers an average intensity of over 1 °C, even if it decreases during the day by 1 °C.

For most sensors the standard deviation varies depending on the daytime, for instance, during the night the deviation is much higher, and the intensity of the temperature can vary around $+ - 2$ °C. However, during the day this deviation is reduced and is therefore more stable, although it is not always at the same time, depending on the sensor, the deviation is narrower during the middle of the day or in the afternoon. This indicates a more homogeneous behavior at midday: when higher temperatures occur, the differences are smaller than in the absence of insolation, indicating differences in heat storage by the surface.

In addition, some sensors near the center of the city present a V-shaped distribution but with a more gradual rise on the right margin, which indicates that during the afternoon the temperature increase is less abrupt. However, they have particularities linked to the specific space within the city in which they are located and not all of them have the same layout, for example S02 or S08. Also noteworthy in the distributions are some of the sensors that have a double valley or descent on the line. Such is the case of S09, S11 or S17; with the presence of vegetation and a distance not very close to the center as a common feature between them.

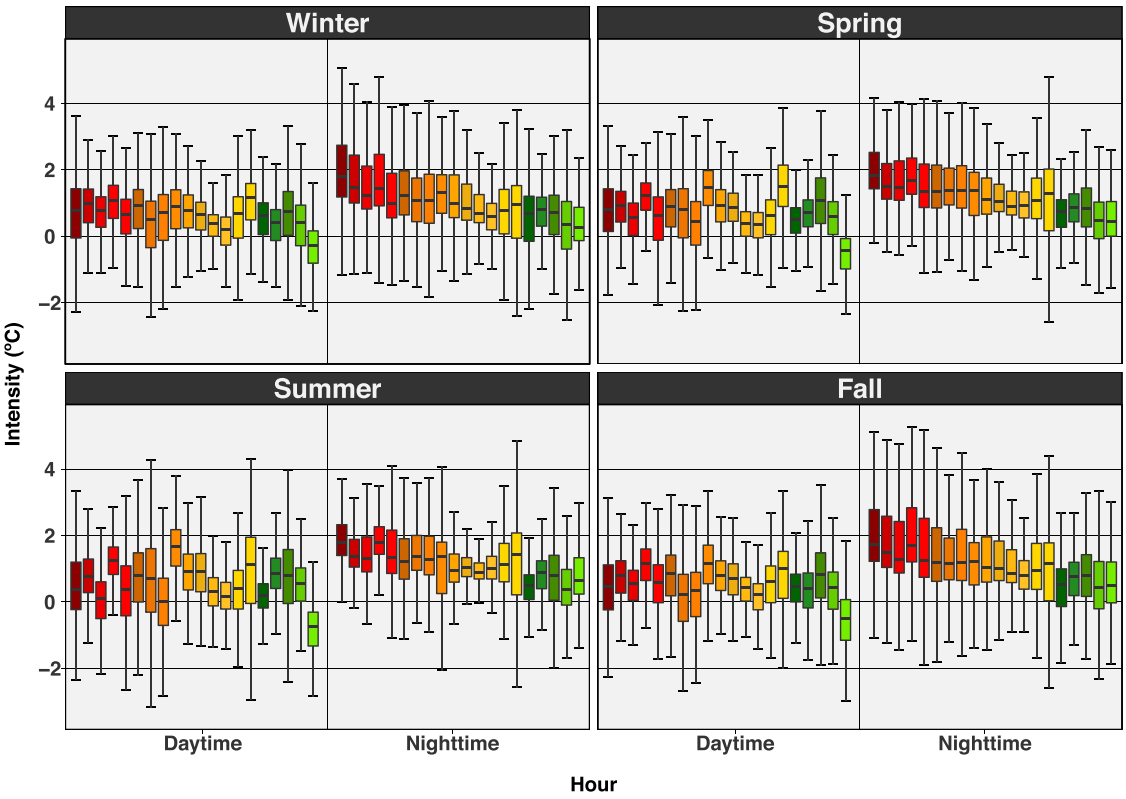

Fig. 9. Boxplot representing daytime (10 h to 18 h) and nighttime (20 h to 6 h) UHI intensity for each season and all sensors in the network, colored according to clustering (Figs. 2 and 8).

With respect to the stations further away from the city or those urban spaces that are large, open spaces with a high presence of vegetation, such as metropolitan parks, the effect of the UHI is lower with an intensity of zero or close to 0 °C. Within this typology, the last row of the graph shows how the effect is so low in some cases that the slight intensities that are reached are recorded during the afternoon and not at night. This is the case of S16, S18 or S19.

The seasonal behavior of UHI (Fig. 9) shows the diurnal (10 h to 18 h) and nocturnal (20 h to 6 h) variation of the intensity for each season of the year and for each sensor of the network.

Results indicate that the intensity of the UHI is higher at night than during the day in all sensors, with values that can reach 2 °C on average above the daytime values. During the night the behavior of the UHI is easily appreciated with a descending gradient of the temperature from the most urban sensors (red colors) to the rural and more distant ones (yellow and green colors), with some exceptions (S15, S16). During the day the behavior of the UHI is diverse depending on the sensor, meaning that the differences between center and periphery are notable during the night and more irregular during the day, depending on the characteristics of the location of each sensor.

In summer, these diurnal differences are the most contrasted within the year and the UHI values may differ from one sensor to another. At night, the UHI intensity is more stable and the ranges become shorter for all sensors concentrating the variability. In the case of autumn and winter, the situation is different and the nighttime UHI values are the highest, with maximum values that in some sensors exceed 4 °C of intensity.

6. Discussion

For the study of urban climate, the use of a city-specific sensor network is an advantage over global or even regional databases, as it allows for a much more detailed description of local-scale climate behavior that is not visible with the use of "general purpose" weather stations such as those of national meteorological services (Muller et al., 2013). These are often located outside urban areas (WMO, 2018) or are such a small number of sites that they are insufficient to analyze the urban environment (Chapman et al., 2015). However, they could fit in UHI studies based on sensor networks, based on adequate validation and comparison allowing a fair comparison regardless of the type of sensor. In contrast, such networks require heavy investment in installation and maintenance, and need to be in operation for a minimum period of time to obtain the first climate characterizations. However, the opportunity offered by these networks to examine urban climate at such a high resolution has led to an increasing number of them being installed (Bassett et al., 2016; Beck et al., 2018; Meier et al., 2017; Núñez-Peiró et al., 2021; Ren et al., 2021; Warren et al., 2016). We must also take into account the size, scale and location of the study city as few medium or small urban areas have such high-density networks as ours (Foissard et al., 2019; Gubler et al., 2021; Moyer and Hawkins, 2017; Skarbit et al., 2017), less so in Mediterranean settings (Martinelli et al., 2020; Pyrgou et al., 2020; Vardoulakis et al., 2013).

In contrast to new technological opportunities, such as the use of satellite data at high spatial and temporal resolution, sensors provide a continuous measurement of air temperature and humidity, rather than surface temperature and humidity (Feng et al., 2021; Voogt and Oke, 2003; Yue et al., 2019) which, although directly related, implies different thermal inertias from those of the air. In addition, this type of continuous measurement by the sensor network allows for an uninterrupted assessment of the UHI by analyzing the diurnal cycle on an hourly basis and its variations, aspects that satellite data and SUHI calculation cannot assess. However, it should also be noted that this continuity in the sensor network is not always perfect and is sometimes altered by sensor registration failures that create information gaps in the time series or erroneous random observations unrelated to the actual observations. This means that this type of network requires greater maintenance of the sensor status and frequency of information download. This requires the development of exhaustive QC to identify errors and eliminate suspicious observations.

Quality control (QC) is a basic part of climate analysis and therefore we have special interest has been given to its application. It allows us to eliminate observations that do not correspond to the natural variability of the climate and, in our case, it has also proved to be an ideal tool for the identification of atmospheric situations (fog, convection, convective precipitation, etc.) that are not included in the usual meteorological monitoring. An application that has not been observed in any other urban climate study of these characteristics and that can be extremely useful in numerical simulations and atmospheric prediction models (Telišman Prtenjak et al., 2018).

The control mainly detects very abrupt outliers that are out of the normal climatic values of the study area, and also more specific outliers related to the joint behavior of the whole network. This is complemented with the study of the hourly variability and synoptic situations in order to specify the search for errors and to detect values that are not really explained by the natural variability of the climate. But sometimes, there are observations related to episodes of disturbance in the sensor record where highly variable fluctuating values are captured that are not identified as errors. Although we know that these observations are in a period in which the sensor registers many errors, the recorded values do not differ from the rest of the values of the network or the sensor itself. Therefore, they are within the natural variability of the network and exceed the QC.

On the other hand, the main limitation of the quality control developed here is that it is not fully automatic. Mainly in the sections of the hourly variability or jump and the calculation of synoptic situations need the direct interpretation of the researcher, reviewing the results obtained and the observations marked as suspicious. This requires some basic knowledge of the sensor network and of the study area to which the quality control is applied. However, this particularity does not affect the extrapolation of this control to any other thermohygrometric sensor network, regardless of scale or location. It is simply necessary to have previous complementary climatic information about the study area, such as average values of maximum and minimum temperature to establish the main thresholds or the annual distribution of precipitation to relate to synoptic situations and explain non-erroneous values. In addition to urban characteristics such as morphology, the density of urbanization, or predominant land cover in the vicinity of the sensors that make up the network. This will also improve the subsequent climatic characterization by explaining certain patterns observed in the

distribution and intensity of the UHI of the different areas.

The exhaustive quality control applied to the database allows the development of a detailed and reliable characterization of the UHI. This characterization has verified how the centre-periphery variation patterns characteristic of the UHI, already observed in many other cities (Alcoforado et al., 2014; Bassett et al., 2016; Beck et al., 2018; Lopes et al., 2013; Núñez-Peiró et al., 2021; Vardoulakis et al., 2013), occur in Zaragoza and in previous works in this same city (Cuadrat Prats et al., 1993, 2005, 2021; Tejedor et al., 2016). Yet on this occasion, and thanks to the large number of sensors in the network and the available hourly resolution, some particularities of the UHI have been analyzed that had not been studied in Zaragoza in such detail until now. For instance, the presence of the urban cold island (UCI) (Acero et al., 2012; Gonçalves et al., 2018), a phenomenon opposite to the UHI with negative intensity values that occurs in urban areas mainly during the morning and is due to the shadows caused by buildings blocking solar radiation and the lack of ventilation (Yang et al., 2017).

The characterization also showed the different magnitudes of intensity that the UHI reaches in the different areas of a city. We were able to characterize not only the most central areas as the warmest, which was already known, but also to differentiate within these areas those which, due to the density of buildings, the urban fabric or the type and material of construction, have the highest intensity values, such as S01 Wome's Centre, S04 Delicias or S05 Oliver. On the other hand, we could also appreciate differences in those places where the UHI effect is lower and observe other conditioning factors beyond the distance to the city center, such as building density, the presence of open spaces, or the presence of vegetation as opposed to built-up impermeable soils. Such is the case of sensor S16 Luis Buñuel Park and S17 Botanical Garden and the importance of urban green infrastructures (Nastran et al., 2019). All these differences between sensors depending on the particularities of the urban space in which they are located make us reflect on the future possibilities of introducing differentiation by LZCs (Stewart and Oke, 2012) in climate characterization. This has a great potential but also certain limitations as the current LCZs models (Bechtel et al., 2015; Demuzere et al., 2019, 2021) are too generalist to be applied in a medium-sized city like Zaragoza.

Finally, the use of a sensor network in the city of Zaragoza allows us to observe differences in the distribution of climate values that would not have been possible with the 3 official stations available. Despite not having long time series, this first approximation serves to characterize the urban areas where the intensity of the UHI is most noticeable, as well as its temporal distribution, both at hourly and seasonal scale. Finally, our results have the potential to be used in urban planning, in the development of strategies for the mitigation of this phenomenon (Akbari and Kolokotsa, 2016; Rizwan et al., 2008), action plans for thermal events of risk to the population (Heaviside et al., 2016, 2017; Taha, 2021) or residential energy planning in cities (Ewing and Rong, 2008; Santamouris, 2016). It is also worth highlighting the potential of this method, together with the implementation of sensor networks, to be replicated in other cities in order to improve the quality of urban climate information. In this way, a sufficiently dense network should be planned to represent all the typical areas of the city, using the LCZs as a basis. Depending on the city and its characteristics, such as urban structure, extension, distribution or its own historical evolution, the number of sensors would vary, but it is necessary that the most characteristic areas are represented by at least one station. Once the network has been implemented, the methodology of the article is easily replicable, which would allow the observations to be refined and detailed urban climate characterizations to be obtained in any city.

7. Conclusions

Using a network of 21 sensors in the city of Zaragoza (Spain) with hourly records of temperature and humidity, a quality control was applied to clean the information and obtain an urban climate database. With this database, a climatic characterization of the UHI was carried out, analyzing the intensity of this phenomenon in different urban areas and the temporal variability of this phenomenon.

The results obtained showed an elimination rate of 1.6% of the recorded observations. Mainly due to errors related to specific outliers and time variability. In addition, the identification of 7 atmospheric situations based on suspicious values by registering an unusual hourly variation (exceeding the network average by 3 sd) allowed the characterization of some typical atmospheric phenomena of the city such as fog, convective storms, etc., which are not recorded in the official climate databases, and which have a determining influence on urban temperature and humidity.

The UHI study revealed that, in the urban areas where there is a high urban density, a greater compactness, and a scarce presence of vegetation cover, the UHI intensity values are higher by around 2 °C, mainly at night. While in these same areas during the morning, the opposite effect occurs, with UCI intensities dropping below 0 °C. Spaces further away from the city center, such as peri-urban neighborhoods, or with a high presence of vegetation, such as urban parks, recorded intensities around 0 °C with little hourly variability, showing a lower influence of the UHI. These center-periphery temperature intensity differences are greater especially during the night and in the winter and autumn seasons, reaching intensities above 4 °C in the most urban sensors.

Funding

This work was supported by the research grant for the recruitment of pre-doctoral research staff in training for the period 2019-2023 (Order IIU/796/2019), from the Departamento de Ciencia, Universidad y Sociedad del Conocimiento of the Diputación General de Aragón.

CRediT authorship contribution statement

Samuel Barrao: Conceptualization, Methodology, Formal analysis, Investigation, Writing – original draft, Writing – review &

editing, Visualization. **Roberto Serrano-Notivoli:** Conceptualization, Methodology, Formal analysis, Investigation, Writing – original draft, Writing – review & editing, Supervision. **José M. Cuadrat:** Investigation, Writing – review & editing, Supervision. **Ernesto Tejedor:** Writing – review & editing. **Miguel A. Saz:** Formal analysis, Investigation, Writing – review & editing, Supervision.

Declaration of Competing Interest

The authors declare that they have no conflict of interest.

Acknowledgements

The authors would like to thank the Department of Medioambiente y Sostenibilidad of the Ayuntamiento de Zaragoza, especially Nieves López and Mariano Aladrén, for their collaboration in the installation and maintenance of the urban sensor network. In addition, the authors are supported by the Government of Aragón through the "Program of Research Groups" (group H09_20R, "Climate, Water, Global Change, and Natural Systems").

References

Acero, J.A., Arrizabalaga, J., Kupski, S., Katzschner, L., 2012. Urban heat island in a coastal urban area in northern Spain. Theor. Appl. Climatol. 1131 (113), 137–154. https://doi.org/10.1007/S00704-012-0774-Z.

Akbari, H., Kolokotsa, D., 2016. Three decades of urban heat islands and mitigation technologies research. Energy Build. 133, 834–842. https://doi.org/10.1016/j.enbuild.2016.09.067.

Alcoforado, M.J., Lopes, A., Alves, E., Canário, P., 2014. Lisbon Heat Island. Finisterra XLIX 61–80.

Arnfield, A.J., 2003. Two decades of urban climate research: a review of turbulence, exchanges of energy and water, and the urban heat island. Int. J. Climatol. 23, 1–26. https://doi.org/10.1002/joc.859.

Bassett, R., Cai, X., Chapman, L., Heaviside, C., Thornes, J.E., Muller, C.L., Young, D.T., Warren, E.L., 2016. Observations of urban heat island advection from a high-density monitoring network. Q. J. R. Meteorol. Soc. 142, 2434–2441. https://doi.org/10.1002/qj.2836.

Bechtel, B., Alexander, P., Böhner, J., Ching, J., Conrad, O., Feddema, J., Mills, G., See, L., Stewart, I., 2015. Mapping local climate zones for a worldwide database of the form and function of cities. ISPRS Int. J. Geo-Inform. 4, 199–219. https://doi.org/10.3390/ijgi4010199.

Beck, C., Straub, A., Breitner, S., Cyrys, J., Philipp, A., Rathmann, J., Schneider, A., Wolf, K., Jacobeit, J., 2018. Air temperature characteristics of local climate zones in the Augsburg urban area (Bavaria, southern Germany) under varying synoptic conditions. Urban Clim. 25, 152–166. https://doi.org/10.1016/j.uclim.2018.04.007.

Chapman, L., Muller, C.L., Young, D.T., Warren, E.L., Grimmond, C.S.B., Cai, X.M., Ferranti, E.J.S., 2015. The birmingham urban climate laboratory: An open meteorological test bed and challenges of the Smart city. Bull. Am. Meteorol. Soc. 96, 1545–1560. https://doi.org/10.1175/BAMS-D-13-00193.1.

Chen, G., Li, X., Liu, X., Chen, Y., Liang, X., Leng, J., Xu, X., Liao, W., Qiu, Y., Wu, Q., Huang, K., 2020. Global projections of future urban land expansion under shared socioeconomic pathways. Nat. Commun. 11, 1–12. https://doi.org/10.1038/s41467-020-14386-x.

Cuadrat Prats, J.M., De la Riva, J., Lopez, F., Marti, A., 1993. El medio ambiente urbano en Zaragoza. Observaciones sobre la "isla de calor.". An. Geogr. la Univ. Complut. 127–138.

Cuadrat Prats, J.M., Vicente Serrano, S., Saz Sánchez, M.Á., 2005. Los efectos de la urbanización en el clima de Zaragoza (España): la isla de calor y sus factores condicionantes. Boletín la Asoc. Geógrafos Españoles 311–327.

Cuadrat Prats, J.M., Serrano-Notivoli, R., Tejedor, E., 2013. Heat and cold waves in Spain. In: García-Legaz, C., Valero, F. (Eds.), Adverse Weather in Spain. AMV EDICIONES, Madrid, pp. 307–324.

Cuadrat Prats, J.M., Saz Sánchez, M.Á., Serrano-Notivoli, R., Tejedor, E., 2014. El clima del término municipal de Zaragoza en el contexto del cambio global, Ayuntamiento de Zaragoza. Agenda 21. Zaragoza.

Cuadrat Prats, J.M., Vicente-Serrano, S., Saz Sánchez, M.Á., 2015. Influence of different factors on relative air humidity in Zaragoza, Spain. Front. Earth Sci. 3, 1–8. https://doi.org/10.3389/feart.2015.00010.

Cuadrat Prats, J.M., Serrano-Notivoli, R., Barrao, S., Saz Sánchez, M.Á., Tejedor, E., 2021. Temporal variability of the urban heat island in Zaragoza (Spain). Cuad. Investig. Geográfica 0. https://doi.org/10.18172/CIG.5022.

de España, Gobierno, 2018. Plan Nacional de Ortofotografía Aérea [WWW Document]. Plan Nac. Obs. del Territ. URL. https://pnoa.ign.es/productos (accessed 9.15.21).

Deilami, K., Kamruzzaman, M., Liu, Y., 2018. Urban heat island effect: A systematic review of spatio-temporal factors, data, methods, and mitigation measures. Int. J. Appl. Earth Obs. Geoinf. https://doi.org/10.1016/j.jag.2017.12.009.

Demuzere, M., Bechtel, B., Middel, A., Mills, G., 2019. Mapping Europe into local climate zones. PLoS One 14, 1–2. https://doi.org/10.1371/journal.pone.0214474.

Demuzere, M., Kittner, J., Bechtel, B., 2021. LCZ generator: a web application to create local climate zone maps. Front. Environ. Sci. 9 https://doi.org/10.3389/fenvs.2021.637455.

Díaz Jiménez, J., García-Herrera, R., Trigo, R.M., Linares Gil, C., Valente, M.A., De Miguel, J.M., Hernández, E., 2006. The impact of the summer 2003 heat wave in Iberia: How should we measure it? Int. J. Biometeorol. 50, 159–166. https://doi.org/10.1007/s00484-005-0005-8.

Durre, I., Vose, R.S., Wuertz, D.B., 2008. Robust automated quality assurance of radiosonde temperatures. J. Appl. Meteorol. Climatol. 47, 2081–2095. https://doi.org/10.1175/2008JAMC1809.1.

EEA, 2018. Urban Atlas 2018 — Copernicus Land Monitoring Service [WWW Document]. Copernicus. URL. https://land.copernicus.eu/local/urban-atlas/urban-atlas-2018 (accessed 9.15.21).

Ewing, R., Rong, F., 2008. The impact of urban form on U.S. residential energy use. Hous. Policy Debate 19, 1–30. https://doi.org/10.1080/10511482.2008.9521624.

Feng, J.L., Cai, X.M., Chapman, L., 2021. A tale of two cities: The influence of urban meteorological network design on the nocturnal surface versus canopy heat island relationship in Oklahoma City, OK, and Birmingham, UK. Int. J. Climatol. 41, E445–E462. https://doi.org/10.1002/joc.6697.

Foissard, X., Dubreuil, V., Quénol, H., 2019. Defining scales of the land use effect to map the urban heat island in a mid-size European city: Rennes (France). Urban Clim. 29, 100490 https://doi.org/10.1016/J.UCLIM.2019.100490.

García-Herrera, R., Díaz Jiménez, J., Trigo, R.M., Luterbacher, J., Fischer, E.M., 2010. A review of the european summer heat wave of 2003. Crit. Rev. Environ. Sci. Technol. https://doi.org/10.1080/10643380802238137.

Garrabou, J., Coma, R., Bensoussan, N., Bally, M., Chevaldonné, P., Cigliano, M., Diaz, D., Harmelin, J.G., Gambi, M.C., Kersting, D.K., Ledoux, J.B., Lejeusne, C., Linares Gil, C., Marschal, C., Pérez, T., Ribes, M., Romano, J.C., Serrano, E., Teixido, N., Torrents, O., Zabala, M., Zuberer, F., Cerrano, C., 2009. Mass mortality in Northwestern Mediterranean rocky benthic communities: effects of the 2003 heat wave. Glob. Chang. Biol. 15, 1090–1103. https://doi.org/10.1111/j.1365-2486.2008.01823.x.

Gonçalves, A., Ornellas, G., Ribeiro, A.C., Maia, F., Rocha, A., Feliciano, M., 2018. Urban Cold and Heat Island in the City of Bragança (Portugal). Clim. 6, 70–76. https://doi.org/10.3390/CLI6030070.

Gubler, M., Christen, A., Remund, J., Brönnimann, S., 2021. Evaluation and application of a low-cost measurement network to study intra-urban temperature differences during summer 2018 in Bern, Switzerland. Urban Clim. 37 https://doi.org/10.1016/j.uclim.2021.100817.
Heaviside, C., Vardoulakis, S., Cai, X., 2016. Attribution of mortality to the urban heat island during heatwaves in the West Midlands, UK. Environ. Health 151 (15), 49–59. https://doi.org/10.1186/S12940-016-0100-9.
Heaviside, C., Macintyre, H., Vardoulakis, S., 2017. The urban heat island: implications for health in a changing environment. Curr. Environ. Heal. Rep. 4, 296–305. https://doi.org/10.1007/s40572-017-0150-3.
Honjo, T., Yamato, H., Mikami, T., Grimmond, C.S.B., 2015. Network optimization for enhanced resilience of urban heat island measurements. Sustain. Cities Soc. 19, 319–330. https://doi.org/10.1016/j.scs.2015.02.004.
Huang, X., Wang, Y., 2019. Investigating the effects of 3D urban morphology on the surface urban heat island effect in urban functional zones by using high-resolution remote sensing data: A case study of Wuhan, Central China. ISPRS J. Photogramm. Remote Sens. 152, 119–131. https://doi.org/10.1016/J.ISPRSJPRS.2019.04.010.
Iñiguez, C., Royé, D., Tobías, A., 2021. Contrasting patterns of temperature related mortality and hospitalization by cardiovascular and respiratory diseases in 52 Spanish cities. Environ. Res. 192, 110191 https://doi.org/10.1016/J.ENVRES.2020.110191.
Instituto Geográfico Nacional, 2012. Límites municipales, provinciales y autonómicos [WWW Document]. Org. autónoma Cent. Nac. Inf. Geográfica. URL. https://www.ign.es/web/ign/portal (accessed 9.15.21).
Laaidi, K., Zeghnoun, A., Dousset, B., Bretin, P., Vandentorren, S., Giraudet, E., Beaudeau, P., 2012. The impact of heat islands on mortality in Paris during the august 2003 heat wave. Environ. Health Perspect. 120, 254. https://doi.org/10.1289/EHP.1103532.
Lemus-Canovas, M., Lopez-Bustins, J.A., Martin-Vide, J., Royé, D., 2019. synoptReg: An R package for computing a synoptic climate classification and a spatial regionalization of environmental data. Environ. Model. Softw. 118, 114–119. https://doi.org/10.1016/j.envsoft.2019.04.006.
Lopes, A., Alves, E., Alcoforado, M.J., Machete, R., 2013. Lisbon urban heat island updated: new highlights about the relationships between thermal patterns and wind regimes. Adv. Meteorol. 2013 https://doi.org/10.1155/2013/487695.
Lott, J.N., 2004. The quality control of the integrated surface hourly database. Proc. Bull. Am. Meteorol. Soc. 5039–5045.
Martinelli, A., Kolokotsa, D.-D., Fiorito, F., 2020. Urban heat island in mediterranean coastal cities: the case of Bari (Italy). Clim. 2020 8, 798. https://doi.org/10.3390/CLI8060079.
Masson, V., Bougeault, P., 1996. Numerical simulation of a low-level wind created by complex orography: a cierzo case study. Mon. Weather Rev. 124, 701–715. https://doi.org/10.1175/1520-0493(1996)124<0701:NSOALL>2.0.CO;2.
Masson, V., Lemonsu, A., Hidalgo, J., Voogt, J., 2020. Urban climates and climate change. Annu. Rev. Environ. Resour. 45, 411–444. https://doi.org/10.1146/annurev-environ-012320-083623.
Meier, F., Fenner, D., Grassmann, T., Otto, M., Scherer, D., 2017. Crowdsourcing air temperature from citizen weather stations for urban climate research. Urban Clim. 19, 170–191. https://doi.org/10.1016/j.uclim.2017.01.006.
Menne, M.J., Durre, I., Vose, R.S., Gleason, B.E., Houston, T.G., 2012. An overview of the global historical climatology network-daily database. J. Atmos. Ocean. Technol. 29, 897–910. https://doi.org/10.1175/JTECH-D-11-00103.1.
Ministerio de Transporte, M. Y A.U, 2021. Áreas urbanas en españa 2020 doi:796-21-023-3.
Moyer, A.N., Hawkins, T.W., 2017. River effects on the heat island of a small urban area. Urban Clim. 21, 262–277. https://doi.org/10.1016/J.UCLIM.2017.07.004.
Muller, C.L., Chapman, L., Grimmond, C.S.B., Young, D.T., Cai, X., 2013. Sensors and the city: a review of urban meteorological networks. Int. J. Climatol. 33, 1585–1600. https://doi.org/10.1002/joc.3678.
Nastran, M., Kobal, M., Eler, K., 2019. Urban heat islands in relation to green land use in European cities. Urban For. Urban Green. 37, 33–41. https://doi.org/10.1016/J.UFUG.2018.01.008.
Núñez-Peiró, M., Sánchez-Guevara Sánchez, C., Neila González, F.J., 2021. Hourly evolution of intra-urban temperature variability across the local climate zones. The case of Madrid. Urban Clim. 39 https://doi.org/10.1016/j.uclim.2021.100921.
Observatorio Municipal de Estadística, 2021. Cifras de Zaragoza. Datos demográficos obtenidos del padrón municipal de habitantes., Excmo. Ayu. ed, Revista Cifras de Zaragoza. Zaragoza.
Oke, T., 1973. City size and the urban heat island. Atmos. Environ. 7, 769–779. https://doi.org/10.1016/0004-6981(73)90140-6.
Oke, T., 1982. The energetic basis of the urban heat island. Q. J. R. Meteorol. Soc. 108, 1–24. https://doi.org/10.1002/qj.49710845502.
Olcina Cantos, J., Serrano-Notivoli, R., Miró, J., Meseguer-Ruiz, O., 2019. Tropical nights on the Spanish Mediterranean coast, 1950-2014. Clim. Res. 78, 225–236. https://doi.org/10.3354/cr01569.
Peng, J., Jia, J., Liu, Y., Li, H., Wu, J., 2018. Seasonal contrast of the dominant factors for spatial distribution of land surface temperature in urban areas. Remote Sens. Environ. 215, 255–267. https://doi.org/10.1016/J.RSE.2018.06.010.
Pyrgou, A., Hadjinicolaou, P., Santamouris, M., 2020. Urban-rural moisture contrast: regulator of the urban heat island and heatwaves' synergy over a mediterranean city. Environ. Res. 182, 109102 https://doi.org/10.1016/J.ENVRES.2019.109102.
Ren, C., Wang, K., Shi, Y., Kwok, Y.T., Morakinyo, T.E., Lee, T., Li, Y., 2021. Investigating the urban heat and cool island effects during extreme heat events in high-density cities: a case study of Hong Kong from 2000 to 2018. Int. J. Climatol. https://doi.org/10.1002/JOC.7222.
Rizwan, A.M., Dennis, L.Y.C., Liu, C., 2008. A review on the generation, determination and mitigation of Urban Heat Island. J. Environ. Sci. 20, 120–128. https://doi.org/10.1016/S1001-0742(08)60019-4.
Romero Rodríguez, L., Sánchez Ramos, J., Sánchez de la Flor, F.J., Álvarez Domínguez, S., 2020. Analyzing the urban heat Island: comprehensive methodology for data gathering and optimal design of mobile transects. Sustain. Cities Soc. 55, 102027 https://doi.org/10.1016/j.scs.2020.102027.
Royé, D., Codesido, R., Tobías, A., Taracido, M., 2020. Heat wave intensity and daily mortality in four of the largest cities of Spain. Environ. Res. 182 https://doi.org/10.1016/j.envres.2019.109027.
Royé, D., Sera, F., Tobías, A., Lowe, R., Gasparrini, A., Pascal, M., De'Donato, F., Nunes, B., Teixeira, J.P., 2021. Effects of Hot Nights on Mortality in Southern Europe. Epidemiology 487–498. https://doi.org/10.1097/EDE.0000000000001359.
Rozenblat, C., Cicille, P., 2004. Les villes européennes: analyse comparative. W@terfront. Public Art.Urban Des. Particip. Regen. 0, 1–94.
Salvati, A., Monti, P., Coch Roura, H., Cecere, C., 2019. Climatic performance of urban textures: analysis tools for a Mediterranean urban context. Energy Build. 185, 162–179. https://doi.org/10.1016/J.ENBUILD.2018.12.024.
Santamouris, M., 2016. Innovating to zero the building sector in Europe: Minimising the energy consumption, eradication of the energy poverty and mitigating the local climate change. Sol. Energy 128, 61–94. https://doi.org/10.1016/j.solener.2016.01.021.
Saz Sánchez, M.Á., Vicente-Serrano, S., Serrano, J., Prats, C., 2003. Spatial patterns estimation of urban heat island of Zaragoza (Spain) using GIS. In: 5th Int. Conf. Urban Clim, 4.
Serrano-Notivoli, R., Beguería, S., Saz Sánchez, M.Á., Longares, L.A., De Luis, M., 2017. SPREAD: a high-resolution daily gridded precipitation dataset for Spain-an extreme events frequency and intensity overview. Earth Syst. Sci. Data 9, 721–738. https://doi.org/10.5194/essd-9-721-2017.
Serrano-Notivoli, R., Beguería, S., De Luis, M., 2019. STEAD: a high-resolution daily gridded temperature dataset for Spain. Earth Syst. Sci. Data 11, 1171–1188. https://doi.org/10.5194/essd-11-1171-2019.
Seto, K.C., Sánchez-Rodríguez, R., Fragkias, M., 2010. The new geography of contemporary urbanization and the environment. Annu. Rev. Environ. Resour. 35, 167–194. https://doi.org/10.1146/annurev-environ-100809-125336.
Skarbit, N., Stewart, I.D., Unger, J., Gál, T., 2017. Employing an urban meteorological network to monitor air temperature conditions in the 'local climate zones' of Szeged, Hungary. Int. J. Climatol. 37, 582–596. https://doi.org/10.1002/JOC.5023.
Smoliak, B.V., Snyder, P.K., Twine, T.E., Mykleby, P.M., Hertel, W.F., 2015. Dense network observations of the Twin Cities Canopy-Layer urban heat island. J. Appl. Meteorol. Climatol. 54, 1899–1917. https://doi.org/10.1175/JAMC-D-14-0239.1.
Stewart, I., 2011. A systematic review and scientific critique of methodology in modern urban heat island literature. Int. J. Climatol. 31, 200–217. https://doi.org/10.1002/joc.2141.

Stewart, I., Oke, T., 2012. Local climate zones for urban temperature studies. Bull. Am. Meteorol. Soc. 93, 1879–1900. https://doi.org/10.1175/BAMS-D-11-00019.1.
Taha, H., 2021. Development of an urban heat mitigation plan for the greater Sacramento Valley, California, a Csa Koppen climate type. Sustain. 13, 1–47. https://doi.org/10.3390/su13179709.
Tejedor, E., Cuadrat Prats, J.M., Saz Sánchez, M.Á., Serrano-Notivoli, R., López, N., Aladrén, M., 2016. Islas de calor y confort térmico en Zaragoza durante la ola de calor de julio de 2015, in: Olcina Cantos, Jorge; Rico Amorós, Antonio M.; Moltó Mantero, E. (Ed.), Clima, Sociedad, Riesgos y Ordenación Del Territorio. Servicio de Publicaciones de la Universidad de Alicante, Sevilla, pp. 141–151. doi:10.14198/XCongresoAECAlicante2016-13.
Telišman Prtenjak, M., Klaić, M., Jeričević, A., Cuxart, J., 2018. The interaction of the downslope winds and fog formation over the Zagreb area. Atmos. Res. 214, 213–227. https://doi.org/10.1016/j.atmosres.2018.08.001.
Tomas-Burguera, M., Jiménez Castañeda, A., Luna Rico, M.Y., Morata, A., Vicente-Serrano, S., González-Hidalgo, J.C., Beguería, S., 2016. Control de calidad de siete variables del banco nacional de datos de AEMET. In: Clima, Sociedad, Riesgos y Ordenación Del Territorio. Servicio de Publicaciones de la UA, Sevilla, pp. 407–415. https://doi.org/10.14198/XCongresoAECAlicante2016-38.
Tsin, P.K., Knudby, A., Krayenhoff, E.S., Ho, H.C., Brauer, M., Henderson, S.B., 2016. Microscale mobile monitoring of urban air temperature. Urban Clim. 18, 58–72. https://doi.org/10.1016/j.uclim.2016.10.001.
United Nations, 2019. World Urbanization Prospects: The 2018 Revision. Department of Economic and Social Affairs, Population Division (ST/ESA/SER.A/420). United Nations.
Vardoulakis, E., Karamanis, D., Fotiadi, A., Mihalakakou, G., 2013. The urban heat island effect in a small Mediterranean city of high summer temperatures and cooling energy demands. Sol. Energy 94, 128–144. https://doi.org/10.1016/j.solener.2013.04.016.
Velleman, P., Hoaglin, D., 1981. Applications, Basics, and Computing of Exploratory Data Analysis. Duxbury Press, Duxbury Press, Boston.
Vicente Serrano, S.M., Cuadrat Prats, J.M., Saz Sánchez, M.Á., 2005. Spatial patterns of the urban heat island in Zaragoza (Spain). Clim. Res. 30, 61–69. https://doi.org/10.3354/cr030061.
Voogt, J., Oke, T., 2003. Thermal remote sensing of urban climates. Remote Sens. Environ. 86, 370–384. https://doi.org/10.1016/S0034-4257(03)00079-8.
Warren, E.L., Young, D.T., Chapman, L., Muller, C., Grimmond, C.S.B., Cai, X., 2016. The Birmingham urban climate laboratory-a high density, urban meteorological dataset, from 2012-2014. Sci. Data 3, 1–8. https://doi.org/10.1038/sdata.2016.38.
WMO, 2017. Guide to the Global Observing System., WMO-No. 488, WMO-No. 488. WMO, Geneva.
WMO, 2018. Guide to Instruments and Methods of Observation, Measurement of Meteorological Variables. WMO, Geneva, p. WMO-No. 8.
Yang, X., Li, Y., Luo, Z., Chan, P.W., 2017. The urban cool island phenomenon in a high-rise high-density city and its mechanisms. Int. J. Climatol. 37, 890–904. https://doi.org/10.1002/JOC.4747.
Yue, W., Liu, X., Zhou, Y., Liu, Y., 2019. Impacts of urban configuration on urban heat island: an empirical study in China mega-cities. Sci. Total Environ. 671, 1036–1046. https://doi.org/10.1016/J.SCITOTENV.2019.03.421.
Zdanowska, N., Rozenblat, C., Pumain, D., 2020. Evolution of urban hierarchies under globalization in Western and Eastern Europe. Reg. Stat. 10, 3–26. https://doi.org/10.15196/RS100202.